Supporting Information

Buey et al. 10.1073/pnas.1713698114

SI Materials and Methods

Protein Production and Purification. gll2934 (*Gloeobacter violaceus*) and slr0600 (*Synechocystis* sp. PCC6803) ORFs were inserted into the pET28a expression vector (Novagen). *Gloeobacter violaceus* Trx-m, EcNTR, and Trx were prepared as described previously (17). Point mutations were performed according to ref. 40. All constructs were corroborated by DNA sequencing. Recombinant proteins were produced in the Rosetta(DE3) *E. coli* cell strain and were purified from the soluble fraction using Ni^{2+} HiPrep (GE Healthcare). The affinity tag was removed with thrombin. Proteins were further purified by gel filtration chromatography on a HiPrep 16/60 Sephacryl S300 (GE Healthcare) in buffer containing 50 mM Tris·HCl (pH 7.6), 150 mM NaCl, and 2 mM β-mercaptoethanol. Flavoproteins were incubated with an excess of FAD (Sigma) before gel filtration, unless otherwise indicated. Selenomethionine (SeMet) protein was expressed in new minimal medium (41), and purification was performed following a procedure similar to that used for the native protein. Protein concentration was measured by the Bradford method (42).

Enzyme Assays. NAD(P)H-dependent TR activity was determined following the reduction of DTNB by measuring the increase in absorbance at 412 nm (21). The assay mixture contained 0.15 mM NAD(P)H, 5 mM DTNB, and 250 nM TR in 100 mM potassium phosphate, 2 mM EDTA, pH 7.0; when the assay was performed in the presence of Trx (5 μM), the concentration of TR was reduced to 50 nM. DTH reduction experiments were performed anaerobically under a nitrogen atmosphere in buffer containing 100 mM potassium phosphate (pH 6.8), 100 mM KCl, and 2 mM EDTA (20). Reduction of flavoproteins (0.05 mM) was monitored in a spectrophotometer after the addition of 0.5 mM DTH (Sigma). At the indicated time, 0.1 mM Trx was added to the reaction mixture, and the flavin spectrum was immediately recorded. EcNTR that is active with its homologous Trx (EcTrx) as well as GvTrx-m served as control (data are shown in ref. 17). Flavin reduction by monothiols (GSH and 2-ME) and dithiols (DTT) was tested by incubating 0.05–0.1 mM of the protein with 10 mM thiol. Spectral changes were recorded 5 min after the addition of the thiol at 25 °C. Oxygen consumption was monitored at 25 °C in a Clark-type oxygen electrode using air-saturated buffer (20 mM KPi, 2 mM EDTA, pH 7.2). The assay mixture contained 100 nM flavoprotein; the reaction was started by the addition of an excess of thiols (1 mM DTT or GSH) over dissolved oxygen (~0.24 mM). A background trace followed the nonenzymatic oxidation of thiol without the addition of enzyme.

ITC. Standard ITC experiments were performed using an AutoiTC200 system (MicroCal). Briefly, a 20-μM enzyme solution in buffer (100 mM potassium phosphate, 2 mM EDTA, pH 7.0) was titrated at 25 °C with a 300-μM AADP solution. A control experiment was performed by injecting the coenzyme into the buffer. The heats of dilution were negligible. The resulting heats were integrated and normalized by the amount of ligand injected. Nucleotide pyridine binding of $AADP^+$ to EcNTR was used as control (data are shown in ref. 17).

Crystallization and Structure Determination. Proteins in buffer containing 10 mM Tris·HCl (pH 7.6) and 50 mM NaCl were concentrated to 20 mg/mL. Protein crystals were grown at room temperature using the vapor-diffusion method by mixing the protein solution with an equal volume of mother liquor. SynDDOR-SeMet protein crystals were obtained with 0.1 M Bis-Tris propane (pH 7.5), 0.2 M sodium sulfate, and 20% (wt/vol) PEG-3350. Crystals of SynDDOR protein, which was not saturated with added FAD, were obtained with 0.03 M sodium phosphate dibasic dihydrate, 0.03 M sodium nitrate, 0.03 M ammonium sulfate, 0.1 M imidazole/Mes (pH 6.5), 20% (vol/vol) poly(ethylene glycol) methyl ether 500, and 10% (wt/vol) PEG 20000. GvDDOR crystals were obtained in 1.5 M lithium sulfate, 0.1 M Na Hepes (pH 7.5). For the GSH:GvDDOR complex, crystals of GvDDOR were soaked in 5 mM GSH. All crystals were immersed in Paratone-N (Hampton Research) for cryoprotection before flash freezing in liquid nitrogen. The structure of SynDDOR-SeMet was phased with a single-wavelength Se anomalous dispersion experiment using HKL2MAP/*SHELX* (43, 44). Diffraction data for GvDDOR were severely anisotropic and were processed using the autoPROC toolbox (45), which makes use of the STARANISO software to deal with anisotropy (46). The STARANISO protocol produced a best-resolution limit of 2.20 Å and a worst-resolution limit of 3.23 Å. The structures of native SynDDOR and GvDDOR and of the GvDDOR:GSH complex were solved by molecular replacement by Phaser (47), using SynDDOR-SeMet as template. The structures were refined using the Phenix crystallographic software suite (48), alternating with visual inspection of the electron density maps and manual modeling with Coot (49). Rigid body, gradient-driven positional, simulated annealing, and restrained individual isotropic B-factor and translation–libration–screw rotation (TLS) (50) were used for structure refinement. The crystallographic and final refinement statistics are summarized in Table S1. The refined structures include most of the SynDDOR and GvDDOR polypeptide chains, with the exception of short, disordered loop regions. Molecular representations were generated using PyMOL version 1.8 (Schrödinger LLC).

Primary Structure Analysis. NTR homologs were collected from the National Center for Biotechnology Information database using *Gloeobacter violaceus* gll2934 and *Synechocystis* sp. PCC 6803 slr0600 as queries by protein blast (e-value less than −95). A protein multiple-sequence alignment was performed using ClustalX (39). Phylogenetic analyses were performed using the MEGA v7.0 software package (51), and the maximum-likelihood method was used for tree reconstruction. The statistical reliability of phylogenetic tree topology was evaluated by bootstrapping with 100 replicates (52).

Growth of Cells and Protein Subcellular Location. *Synechocystis* sp. PCC 6803 cells were grown photoautotrophically on BG11C (53) at 30 °C under continuous illumination (50 $\mu E \cdot m^{-2} \cdot s^{-1}$) and bubbled with a stream of 1% (vol/vol) CO_2 in air. For generation of the SynDDOR–3HA–tagged strain, the slr0600 gene was amplified by overlapping PCR into pGEMT, and a 3HA coding sequence followed by a nourseothricin resistance cassette was inserted to replace the stop codon to generate pDDOR3HA. This plasmid was used to transform a WT strain as described in ref. 54. Cells of exponentially growing cultures were harvested (50 $OD_{750\ nm}$ units), resuspended in a buffer containing 25 mM Hepes·NaOH (pH 7.0), 15 mM $CaCl_2$, 5 mM $MgCl_2$, 15% (vol/vol) glycerol, and 1 mM PMSF (buffer A), and subjected to two cycles of 1-min vortexing in a minibead-beater separated by 5 min on ice. Unbroken cells were removed by centrifugation at 2,300 × *g* for 5 min, and total membranes were then pelleted by centrifugation at 16,000 × *g* for 20 min. The supernatant was centrifuged again, and the second

supernatant constituted the soluble fraction that was further fractionated. The pellet from the first centrifugation was washed twice by resuspension in buffer A and was centrifuged at 16,000 × *g* for 20 min (fraction I). Washed membranes were resuspended in buffer B [20 mM Tris·HCl (pH 8.0), 0.75 M NaCl, and 0.02% (vol/vol) Triton X-100] and were centrifuged at 16,000 × *g*. The supernatant constituted fraction II that contains the proteins extrinsically attached to the membranes. The pellet resuspended in buffer A was considered purified membranes. For immunoblot analysis, proteins were fractionated on SDS/PAGE and immunoblotted with antibodies against the HA tag (Sigma), a membrane component of the nitrate-transporting system (NrtA) (55), and cytosolic glutamine synthetase I (GSI) (56). The ECL Plus immunoblotting system (Amersham) was used to detect the different antigens with anti-rabbit or anti-mouse secondary antibodies conjugated to horseradish peroxidase.

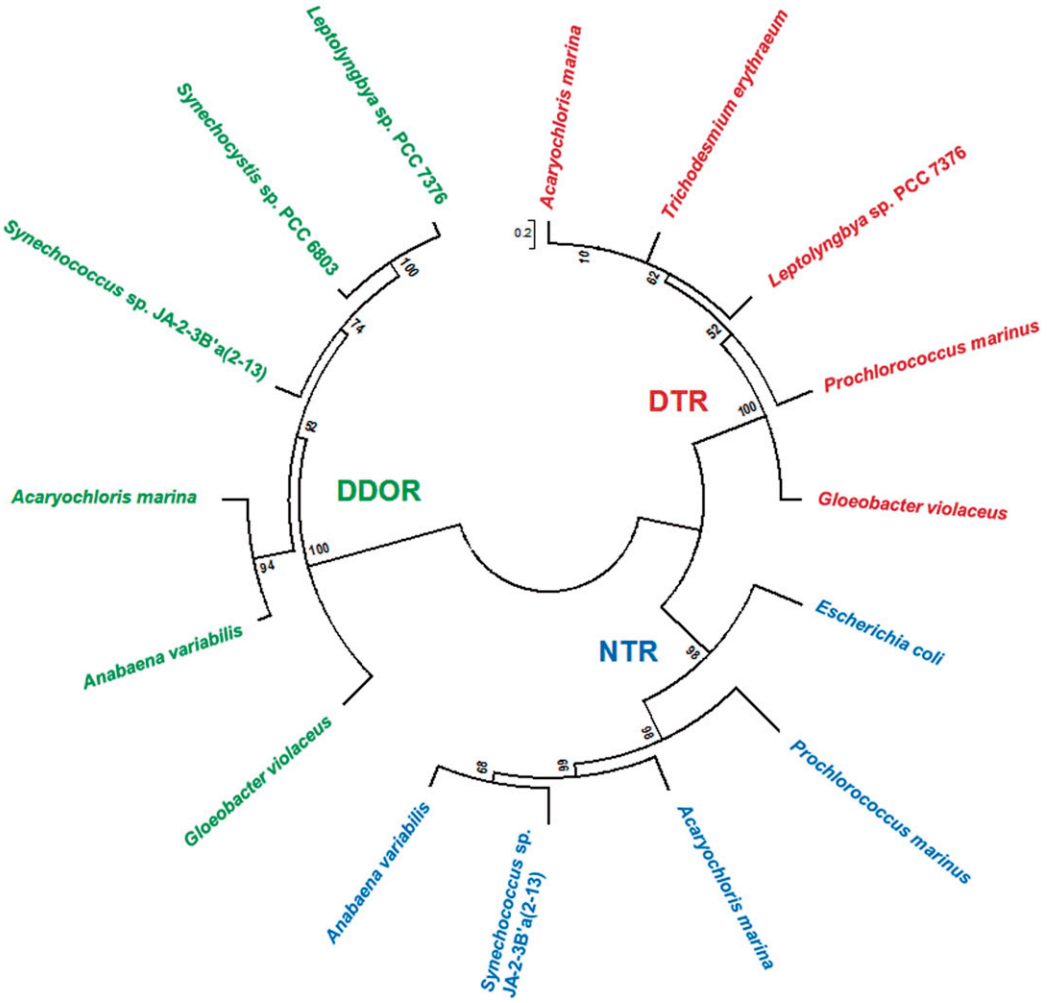

Fig. S1. A maximum-likelihood unrooted phylogenetic tree showing the diversity of NTR-related protein families (NTR/NTRC, DTR, and DDOR) in cyanobacteria. The sequence of EcNTR was included.

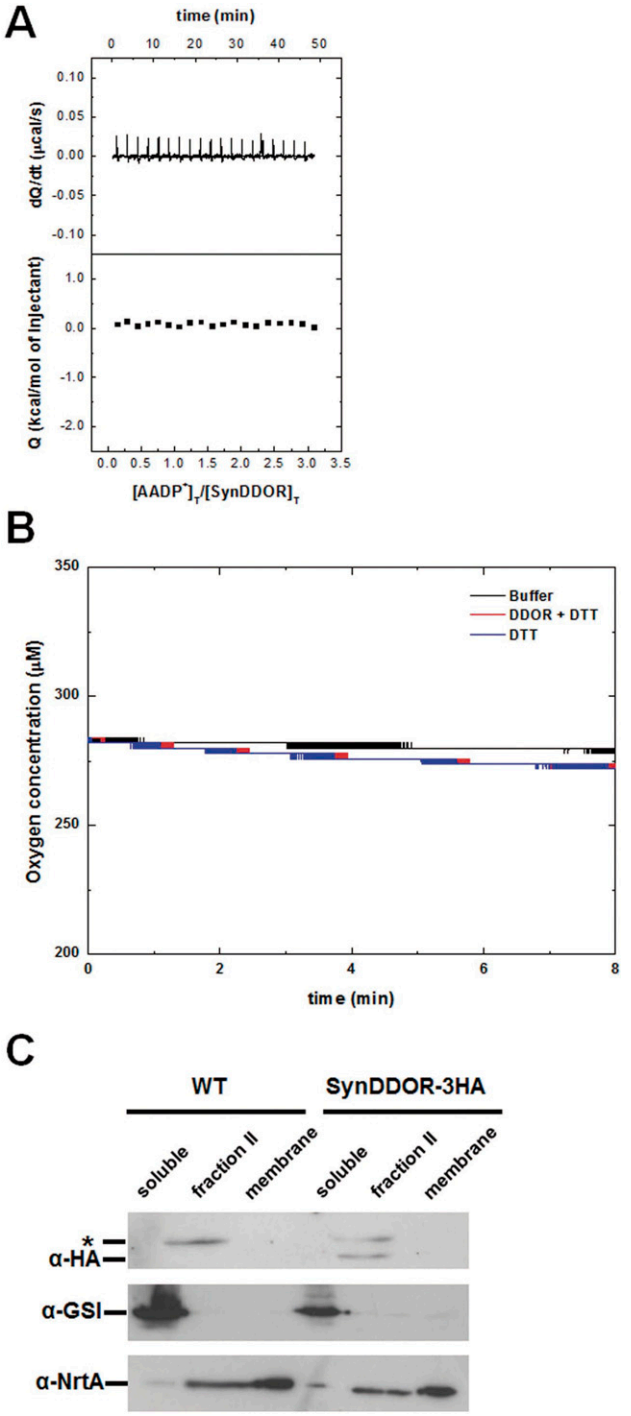

Fig. S2. (*A*) Calorimetric assay for the binding of $AADP^+$ to SynDDOR. (*Upper*) Thermogram corresponding to raw data of heat power release associated with the sequential addition of the ligand ($AADP^+$) to the protein solution. (*Lower*) Binding isotherm (ligand-normalized integrated heats as a function of the molar ratio $[(ligand)_{Total}/(protein)_{Total}]$. (*B*) Oxygen consumption by 100 nM SynDDOR in the presence of an excess of thiols (1 mM DTT or GSH) over dissolved oxygen (~0.24 mM) in buffer [50 mM Tris·HCl (pH 7.6), 150 mM NaCl, 1 mM EDTA]. (*C*) Examination of protein localization by cellular fractionation and Western blot immunodetection. The distribution of DDOR between the membrane and soluble fractions of *Synechocystis* was analyzed by immunoblotting using anti-3HA antibody. Fraction II contains the proteins extrinsically associated with the membranes. Antibodies against GSI (a cytosolic protein) and NrtA (a membrane protein) were used as controls. The asterisk indicates a nonspecific signal.

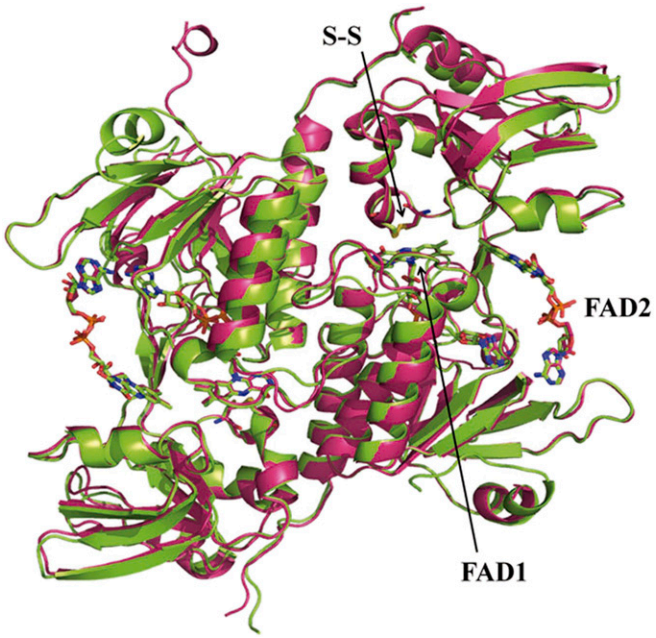

Fig. S3. Superposition of solved structures of a GvDDOR protein crystal (yellow) and SynDDOR (magenta) yields a rmsd value of 0.74 Å. The two amino acid sequences are 63% identical and 77% similar (Fig. 1 in the main text). Cys residues in the CxxC redox motif were found partially oxidized in the crystal structure of GvDDOR.

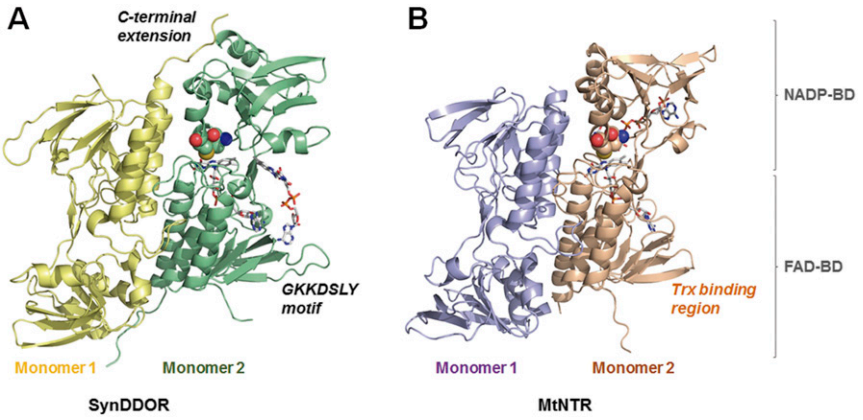

Fig. S4. Structural comparison of (*A*) SynDDOR and (*B*) *Mycobacterium tuberculosis* NTR (MtNTR) in the FO conformation (PDB ID code: 2A87) (57). Homodimers are shown as ribbon models. Each monomer is composed of two domains named "FAD-binding" (FAD-BD) and "NADP-binding" (NADP-BD) domains, respectively, for MtNTR. The figure highlights the structural differences between flavoproteins, particularly in the NADP-BD and the Trx-binding region, as well as the presence of a C-terminal extension in DDOR. Cysteines in the redox-active CxxC motif are shown as spacefill; FAD and NADPH cofactors, in the FAD-BD and NADP-BD, respectively, are shown in stick representation for one of the monomers in MtNTR.

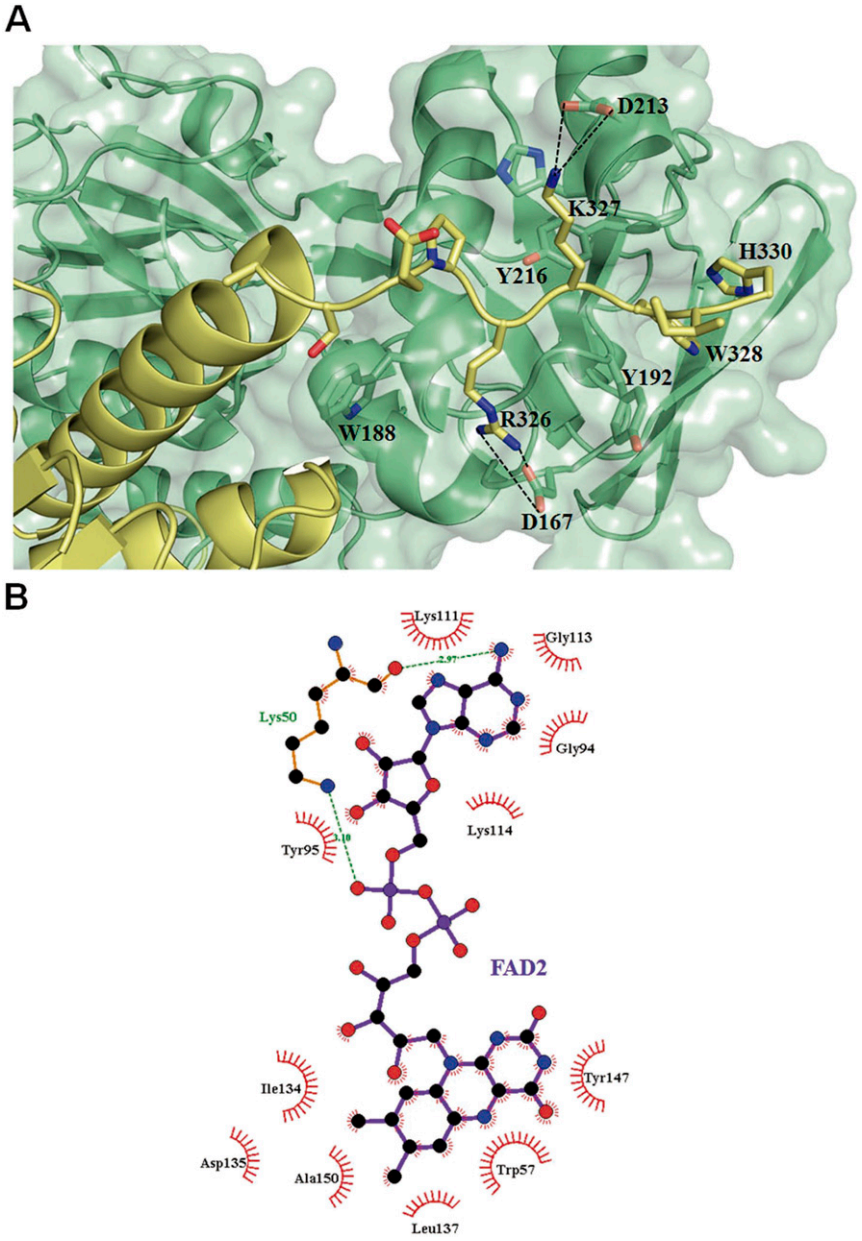

Fig. S5. Schematic diagram of selected atomic interactions in DDOR. (*A*) Residues involved in polar interactions between the C-terminal tail of monomer 1 (yellow) with monomer 2 (green) in SynDDOR as computed by the Pisa server (www.ebi.ac.uk/msd-srv/prot_int/pistart.html). Salt bridges are shown as dashed lines. (*B*) Interactions of FAD2 (cofactor backbone in violet) with amino acid residues of SynDDOR as computed by the Ligplot+ software package (https://www.ebi.ac.uk/thornton-srv/software/LigPlus/). Hydrophobic interactions are shown as red arcs. Hydrogen-bond interactions are represented by green dotted lines with bond distances in Ångstroms. Oxygen atoms are colored red, nitrogen atoms blue, and carbon atoms black.

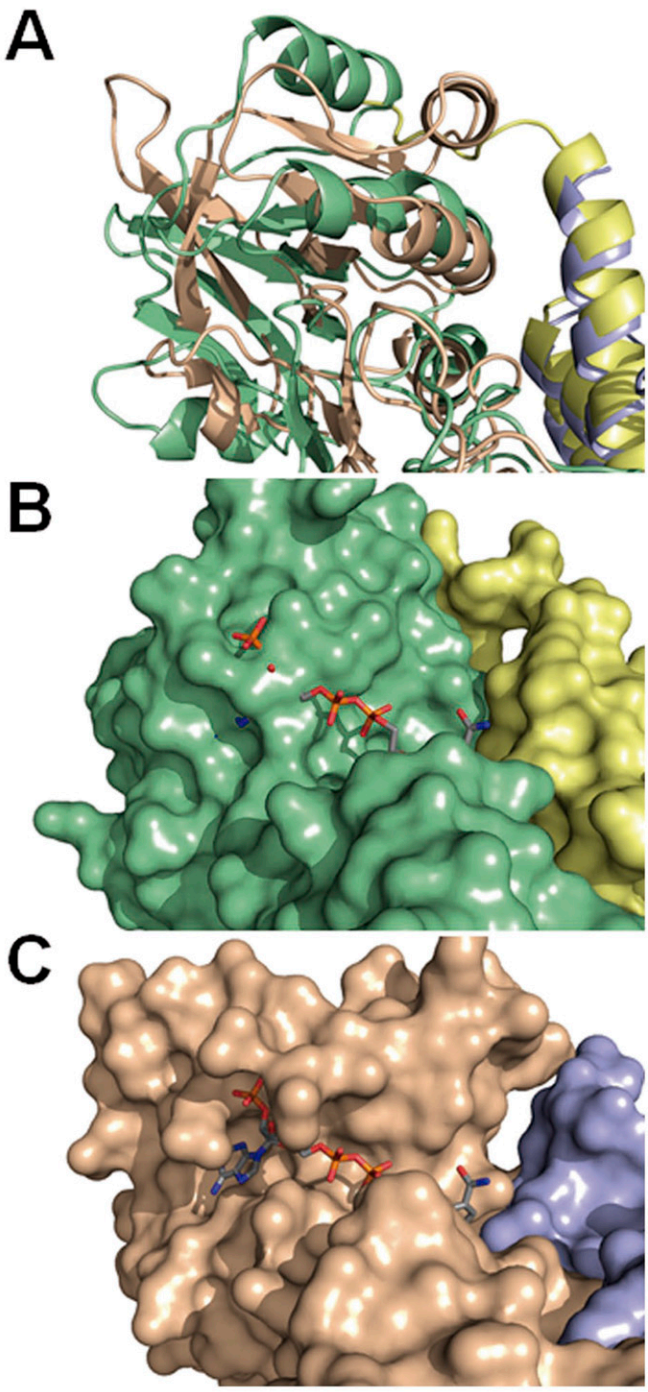

Fig. S6. (*A*) Ribbon representation of SynDDOR and MtNTR NADP-binding domains superimposed (backside of monomer 2 in Fig. S4). (*B*) Model of pyridine nucleotide (in stick representation) docked over the vicinity of the CxxC motif in SynDDOR, shown in molecular surface representation. (*C*) NADPH (in stick representation) in MtNTR (shown in molecular surface representation) as observed in the crystal structure.

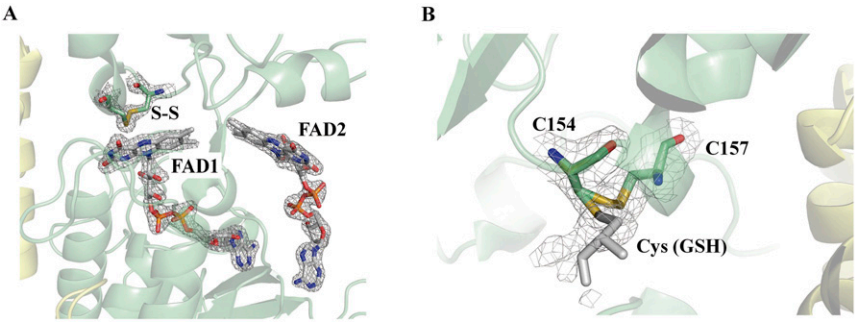

Fig. S7. (*A*) A zoomed-in view of the three redox-active centers in SynDDOR monomer 2 as represented in Fig. 3*A* in the main text. The disulfide and the two FAD cofactors are shown as stick models, and the 2Fo-Fc electron density maps drawn at 1.0 σ contour level are shown as gray mesh. (*B*) In GvDDOR crystals incubated with GHS, an elongated electron density peak prolonging the sulfhydryl group of the CxxC motif is interpreted as a disulfide bridge and a GSH mixed disulfide with partial occupancies (Fig. 3*C* in the main text). Nonetheless, the electron density of the map did not allow the unambiguous modeling of GSH, and thus the coordinates of the thiol are not included in the final model deposited in PDB. The 2Fo-Fc electron density map for the Cys residues is shown at 1.0 σ contour level as a gray mesh.

Table S1. Data collection and refinement statistics

Parameter	SynDDOR SeMet	SynDDOR	GvDDOR	GvDDOR:GSH complex
Diffraction data statistics				
Wavelength, Å	0.9792	0.9999	0.9999	0.9999
Resolution range, Å	49.08–1.95 (2.02–1.95)	46.03–1.71 (1.77–1.71)	55.96–2.20 (2.28–2.20)	48.66–1.95 (2.02–1.95)
Space group	P 2_1 2_1 2_1	P 2_1	I 2 2 2	I 2 2 2
Unit cell, Å/°	71.7 79.3 127.1/ 90.0 90.0 90.0	66.0 128.4 92.7/ 90.0 91.6 90.0	57.2 136.4 267.7/ 90.0 90.0 90.0	57.8 143.3 265.1/ 90.0 90.0 90.0
Total reflections	676,357 (56,347)	1,110,820 (111,315)	479,723 (21,886)	807,463 (78,538)
Unique reflections	101,579 (10,075)	167,283 (16,604)	38,467 (1,912)	80,405 (7,827)
Multiplicity	6.7 (5.6)	6.6 (6.7)	12.5 (11.4)	10.0 (10.0)
Completeness, %	99.7 (98.8)	99.9 (99.6)	96.4 (95.7)*	99.0 (95.7)
Mean I/σ(I)	6.85 (1.17)	12.16 (1.19)	16.8 (2.1)	9.19 (0.88)
Wilson B-factor	26.34	27.09	33.76	37.03
R-pim	0.100 (0.721)	0.042 (0.540)	0.031 (0.325)	0.054 (0.938)
CC1/2	0.994 (0.673)	0.998 (0.609)	0.998 (0.770)	0.997 (0.472)
Refinement statistics				
Resolution, Å	49.08–1.95	46.03–1.71	55.96–2.20	48.66–1.95
R-work	0.21 (0.37)	0.17 (0.34)	0.25 (0.34)	0.20 (0.44)
R-free	0.24 (0.36)	0.19 (0.36)	0.27 (0.39)	0.23 (0.47)
Non-H atoms				
Macromolecules	4,807	9,787	4,974	4,691
Ligands	274	634	267	327
Solvent	421	1,200	262	341
Protein residues	628	1,276	646	623
Rms (bonds)	0.010	0.012	0.008	0.018
Rms (angles)	1.17	1.20	1.03	1.47
Ramachandran, %				
Favored	97.92	98.42	96.70	97.73
Allowed	2.08	1.58	3.30	2.27
Outliers	0.00	0.00	0.00	0.00
Rotamer outliers. %	0.00	0.00	1.83	1.78
Average B-factor	33.99	34.20	50.07	53.86
Macromolecules	33.36	32.40	50.06	52.29
Ligands	38.52	44.46	65.47	74.49
Solvent	38.27	43.43	34.63	55.67
PDB code	5JRI	5K0A	5ODE	5N0J

Statistics for the highest-resolution shell are shown in parentheses. Five percent of reflections were used for calculation of R_{free}.
*Values shown in the table for GvDDOR correspond to STARANISO ellipsoidal completeness. Spherical completeness values are 71.0 (37.8).